Electron Spin Resonance Imaging of Mouse B16 Melanoma

Hiratoshi KATSUDA,*[,a] Tadashi KOBAYASHI,[a] Haruo SAITO,[b] Takayuki MATSUNAGA[b] and Motoji IKEYA[c]

School of Pharmacy, Hokuriku University,[a] 3, Ho Kanagawa-machi, Kanazawa 920-11, Japan, Toyama Prefectural Institute for Pharmaceutical Research,[b] 17-1 Nakataikoyama, Kosugi, Toyama 939-03, Japan and Department of Physics, Osaka University,[c] Toyonaka 560, Japan. *Received March 20, 1990*

An X-band electron spin resonance (ESR) imaging apparatus with a pin-hole TE_{102} mode cavity and a rapid scan coil was constructed. Using this apparatus, ESR imaging of melanin in mouse B16 melanoma was observed for the first time. The ESR spectrum of B16 melanoma is similar to that of natural melanin extracted from sepia officinalis in microwave power dependence.

Keywords ESR; magnetic resonance imaging; pin-hole cavity; X-band; rapid scan; averaging; radical; melanin; B16 melanoma; mouse

Recently an electron spin resonance imaging (ESRI or ESRCT) apparatus has been developed by Ohno,[1] Nishikawa,[2] Ogata *et al.*[3] and Ikeya[4] in Japan. Furusawa and Ikeya have recently developed a pin-hole cavity (resonator) for microwave scanning electron spin resonance (ESR) imaging to be used for ESR dating and dosimetry and to be applied in the field of geoscience.[5] On the other hand, Berliner *et al.* reported ESR imaging of living mouse tumor[6] at L-band frequency using a single-turn flat-loop coil. They used a spin labelling agent (paramagnetic nitroxide, 3-carboxamido-2,2,5,5-tetramethyl-pyrroline-1-oxyl (CTPO)) injected into the tail vein, and a cross-sectional image was obtained perpendicular to the tail axis. The practical application of ESRCT in the biological field is to observe the mechanisms of metabolism, diffusion and transport phenomena.

In the present work, individual parts of the ESR imaging apparatus have been improved one by one for higher accuracy and sensitivity. As one of the applications of this apparatus, the ESR imaging picture of melanin obtained from mouse B16 melanoma is reported.

Experimental

Apparatus In this work the microwave scanning ESR imaging apparatus was developed and improved as follows. The system was constructed using a TE_{102} mode X-band pin-hole cavity, JEOL's JES-FE2XG type ESR spectrometer, JEOL's magnetic field rapid scan unit, *X–Y* sample stage with stepping motors, Panasonic's digital oscilloscope, NF's lock-in amplifier and NEC's personal computer (PC9801VX). Several distinctive features of our ESR imaging apparatus in Fig. 1 are as follows; our ESR sample cavity has a reference sample holder to tune up the microwave unit and to normalize the ESR signal intensity of the sample, internal and external 100 kHz magnetic modulation coils to measure the ESR intensities of the sample and reference at the same time, *X–Y* sample stage controlled by stepping motors to scan the sample step by step on the local pin-hole region of the cavity.

Methods To measure weak ESR signals, JEOL's rapid scan unit has been applied. By using this unit we can attain a high speed magnetic field

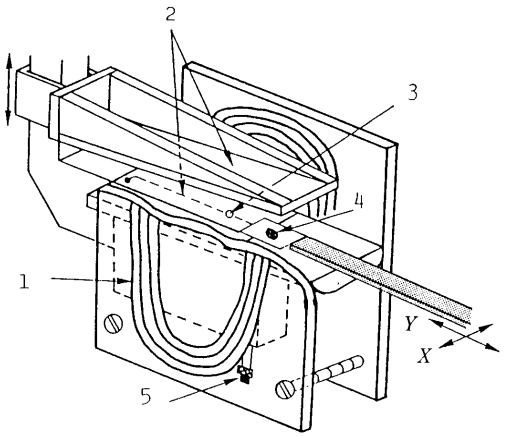

Fig. 1. Schematic Diagram of Imaging Cavity

Our ESR imaging apparatus was constructed using a TE_{102} mode pin-hole cavity at X-band frequency. A reference sample holder was used in the cavity to tune up the microwave unit and to calibrate the magnetic field intensity. The ESR signal intensity of the sample was normalized by comparing it with that of the reference one. Rapid sweeping of the field was made to measure the weak ESR signal by high-speed accumulation. 1, rapid scan coil; 2, 100 kHz modulation coil; 3, pin-hole; 4, sample; 5, reference sample ($MgO:Mn^{2+}$).

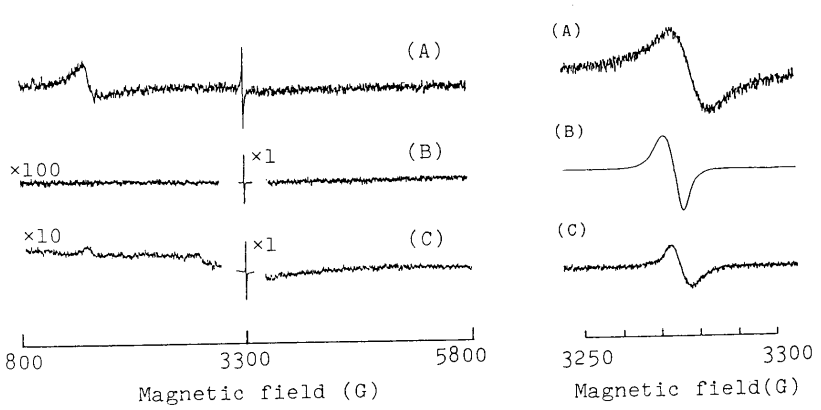

Fig. 2. ESR Spectrum of Melanin

Conditions for the measurement of ESR spectrum for (A) synthetic melanin powder sample: power, 24.5 mW; modulation amplitude, 0.2 G; scan time, 8 min; time constant, 0.1 s; amplitude gain, 10 × 100; temperature, 18 °C. (B) natural melanin powder sample: power, 1.6 mW; modulation amplitude, 0.05 G; scan time, 2 min; time constant, 0.01 s; amplitude gain, 5 × 10; temperature, 18 °C. (C) B16 melanoma sample: power, 5.0 mW; modulation amplitude, 0.2 G; scan time, 8 min; time constant, 0.01 s; amplitude gain, 0.5 × 10; temperature, −39 °C.

sweep and accumulation of ESR spectra. The scanning time is 0.1 s. The ESR signals go through the lock-in amplifier for noise reduction. These signals are accumulated in the digital oscilloscope so that the S/N ratio of ESR spectra can be improved. The accumulated peak-to-peak ESR intensities (*i.e.* measured spin concentration) of the first-differential ESR spectrum of the sample and the reference are automatically measured and these data are led to a personal computer through the GP-IB interface bus. In a similar way the two stepping motors attached to the *X*–*Y* sample stage are controlled by a personal computer. In this way the highly sensitive and fully automatic microwave scanning ESR imaging apparatus was constructed.

Materials Natural and synthetic melanin were purchased from Sigma Chemical Co. The natural one was extracted from sepia officinalis and the synthetic one was prepared by persulfate oxidation of tyrosine. Mouse melanoma (B16-F10) was kindly provided by Prof. K. Miyamoto, Hokuriku University. This cell line was maintained in Eagle's Minimum Essential Medium (Nissui) supplemented with 10% fetal calf serum (M. A. Bioproducts). The cells (10^6 cells) were subcutaneously implanted in the back of the mouse (C57BL). The solid type tumor was removed from the back after 10—14 d and was used for this experiment.

Results and Discussion

Figure 2 shows the ESR spectra measured by a TE_{011} mode cavity. Figure 2(A) and (B) are ESR spectra of synthetic and natural melanin powder samples (20 mg in weight) at 18 °C. The *g*-values are 2.003, 2.004, and line widths are 9.7 G, 5.1 G, respectively. As shown in Fig. 2(A), the synthetic melanin sample contains Fe^{3+} ions. These transition metal ions show the ESR signal at $g=4.3$, the intensity of which is almost equal to the melanin radical signal at $g=2.003$. The line width of the ESR spectrum of the synthetic melanin is twice as large as the natural one because of the bound Fe^{3+} ions. This affects the power saturation phenomenon of the microwave.[7] On the other hand, Fig. 2(C) is the ESR spectrum of the B16 melanoma removed from the back of the mouse. In order to prevent water from decreasing the *Q*-value of the ESR cavity, the ESR spectrum of the B16 melanoma was obtained at −39 °C by the nitrogen gas flow method. The *g*-value is 2.004, and the line width is 7.2 G. Figure 3 shows microwave power dependence of the ESR spectra of synthetic and natural melanins and the B16 melanoma. ESR intensities of natural melanin and B16 melanoma are saturated by microwave power at 1.6 and 3.2 mW, respectively. On the other hand, the synthetic melanin is not saturated in up to 50—100 mW. These experimental results are interpreted as follows; the ESR intensity of pure melanin is easily saturated by the microwave power, on the other hand, the melanin radical centers bound to the metal ions can hardly be saturated as is pointed out by Okazaki *et al.*[7]

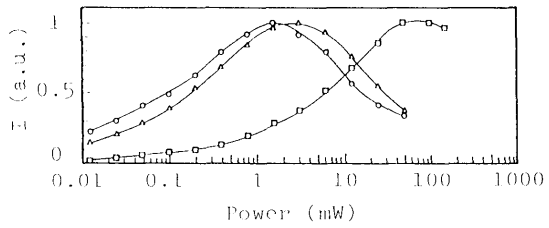

Fig. 3. The Microwave Power Dependence of ESR Intensities of Natural Melanin, Synthetic Melanin and B16 Melanoma

—○—, B16 melanoma; —△—, natural melanin; —□—, synthetic melanin.

The ESR imaging of natural melanin powder is shown in Fig. 4. A cone like hole 2.7 mm in diameter was made on an acrylic resin plate, and was then filled with natural melanin. In order to prevent the sample from dropping out of the hole, the surface was covered with 45 μm thick cellophane tape. The test samples were placed on an *X*–*Y* sample stage. The signal intensities at 31×31 points were measured. The ESR image (A) is shown by 8 levels of shading in proportion to the ESR intensity. (B) and (D) show the projected figures along *X* and *Y* axes, respectively, and (C) is a bird's-eye view on the *X*–*Y* plane. The *Z* axis shows the ESR intensity.

Figure 5 shows the ESR imaging picture of B16 melanoma. The mouse tumor was kept in a desiccator with silica gel in order to dry without reducing the *Q*-value of the ESR cavity. This sample was ground into pieces, and then put on a cover-glass. The cover-glass was set up on an *X*–*Y* sample stage. This ESR image is shown by 6 levels of shading in proportion to the ESR intensity.

Conclusions

ESR imaging of melanin in mouse B16 melanoma was observed using the microwave scanning ESR method at X-band frequency. Distribution of natural melanins (sepia officinalis and mouse B16 melanoma) was imaged on a cathode ray tube (CRT) display. However, the signal intensity of synthetic melanin is too weak to be imaged with

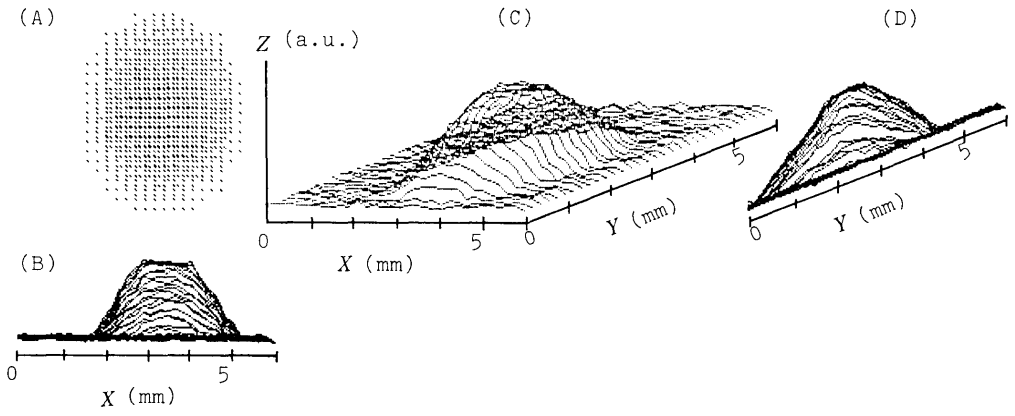

Fig. 4. ESR Imaging Picture of Natural Melanin

The measurement condition was as follows; a small pin-hole 1.5 mm in diameter was made in a 0.05 mm thick silver plate of a TE_{102} mode rectangular cavity. The ESR signal intensities at 31×31 points were measured and are indicated by the shading code. The elements of the ESR imaging picture were measured at equal distances, 0.2 mm, with an *X*–*Y* stage.

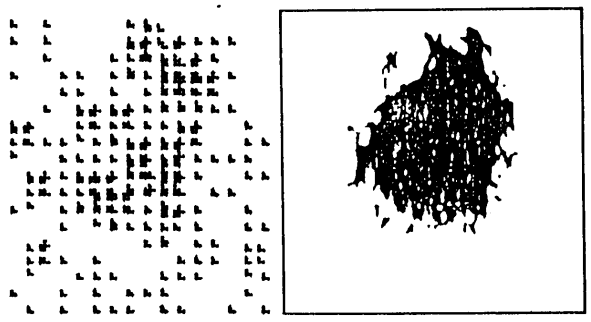

Fig. 5. The ESR Imaging Picture (A) of Melanin Obtained from Mouse B16 Melanoma Removed from the Back of a Mouse with a Sample Habit (B)

A large pin-hole 3.0 mm in diameter was made in a 0.05 mm thick silver plate to measure the ESR imaging picture of the B16 melanoma.

the present apparatus. This method will be used in the study of the assay of other biological samples and in the diagnosis of various diseases.

Acknowledgements We would like to thank Prof. Ken-ichi Miyamoto of Hokuriku University for the gift of mouse B16 melanoma and Mr. Hidemoto Hara of Micro Device Co. for the trial constructions of the ESR imaging apparatus. This work was partially supported by a Grant-in-Aid for Scientific Research from the Ministry of Education, Science and Culture.

References and Notes

1) K. Ohno, *Jpn. J. Appl. Phys.*, **20**, L179 (1981); K. Ohno, *J. Magn. Reson.*, **64**, 109 (1985); K. Ohno and T. Murakami, *ibid.*, **79**, 343 (1988).
2) H. Nishikawa, H. Fujii and L. J. Berliner, *J. Magn. Reson.*, **62**, 79 (1985).
3) T. Ogata, *O plus E*, **113**, 104, (1989).
4) M. Ikeya and T. Miki, *Jpn. J. Appl. Phys.*, **26**, L929 (1987); T. Miki and M. Ikeya, *ibid.*, **26**, L1495 (1987); T. Miki and M. Ikeya, *J. Magn. Reson.*, **80**, 502 (1988).
5) M. Furusawa and M. Ikeya, *Analytical Sciences*, **4**, 649 (1988).
6) L. J. Berliner, H. Fujii, X. Wan and S. J. Lukiewicz, *Magnetic Resonance in Medicine*, **4**, 380 (1987); L. J. Berliner and H. Fujii, *Science*, **227**, 517 (1985).
7) M. Okazaki, K. Kuwata, Y. Miki, S. Shiga and T. Shiga, *Arch. Biochem. Biophys.*, **242**, 197 (1985).